Backbone-Modified C_2-Symmetrical Chiral Bisphosphine TMS-QuinoxP*: Asymmetric Borylation of Racemic Allyl Electrophiles

Hiroaki Iwamoto,[†#] Yu Ozawa,[†#] Yuta Takenouchi,[†] Tsuneo Imamoto,[‡,§] and Hajime Ito[†,∥*]

[†] Division of Applied Chemistry, Graduate School of Engineering, Hokkaido University, Sapporo, Hokkaido 060-8628, Japan

[‡] Organic R&D Department, Nippon Chemical Industrial Co., Ltd., Kameido, Koto-Ku, Tokyo 136-8515, Japan

[§] Department of Chemistry, Graduate School of Science, Chiba University, Yayoi-cho, Inage-ku, Chiba 263-8522, Japan

[∥] Institute for Chemical Reaction Design and Discovery (WPI-ICReDD), Hokkaido University, Sapporo, Hokkaido 060-8628, Japan

KEYWORDS: Chiral bisphosphine ligand, Direct enantioconvergent reaction, Asymmetric borylation, Copper(I)-catalyst, DFT calculation

ABSTRACT: A new C_2-symmetrical P-chirogenic bisphosphine ligand with silyl substituents on the ligand backbone, (*R*,*R*)-5,8-TMS-QuinoxP*, has been developed. This ligand showed higher reactivity and enantioselectivity for the direct enantioconvergent borylation of cyclic allyl electrophiles than its parent ligand, (*R*,*R*)-QuinoxP* (e.g. for a piperidine-type substrate: 95% ee vs. 76% ee). The borylative kinetic resolution of linear allyl electrophiles was also achieved using (*R*,*R*)-5,8-TMS-QuinoxP* (up to 90% ee, *s* = 46.4). An investigation into the role of the silyl groups on the ligand backbone using X-ray crystallography and computational studies displayed interlocking structures between the phosphine and silyl moieties of (*R*,*R*)-5,8-TMS-QuinoxP*. The results of DFT calculations revealed that the entropy effect thermodynamically destabilizes the dormant dimer species in the catalytic cycle to improve the reactivity. Furthermore, in the direct enantioconvergent case, detailed calculations indicated a pronounced enantioselective recognition of carbon–carbon double bonds, which is virtually unaffected by the chirality at the allylic position, as a key for the borylation from both enantiomers of racemic allyl electrophiles.

INTRODUCTION

Chiral bisphosphine ligands have significantly contributed to the evolution of catalytic enantioselective organic transformations.[1–3] For several decades, tremendous effort has been devoted to the development of chiral bisphosphine ligands in order to achieve high enantioselectivity and reactivity for transition-metal catalysis.[4] Careful design of the three-dimensional structures of chiral bisphosphines is required to achieve high enantioselectivity (Figure 1A). The most important factors in the design of chiral bisphosphine ligands are the structure of the backbone and the substituents on the phosphorus atoms. In transition-metal complexes, the bite angle between the two phosphorus atoms, which is crucial to the reactivity and stereo-environment of the catalyst, depends on the backbone structure and the metal center.[5,6] The substituents on the phosphorus atoms are also important for the stereoselectivity, as they interact with the substrates via intermolecular interactions such as steric repulsion and attraction via dispersion forces.[7–9] The chirality of C_2-symmetrical bisphosphine ligands often arises from the backbone structure as in e.g., BINAP and SEGPHOS;[10–12] however, the construction of chiral phosphine moieties, i.e., P-chirogenic centers such as those in DIPAMP and QuinoxP*,[13–16] or the introduction of chiral motifs on the phosphorus atom in e.g. Me-Duphos are also powerful approaches (Figure 1B).[17–19] Further improvement of chiral bisphosphine ligands to achieve higher enantioselectivity has also been attempted via optimization of the substituents on the phosphorus atoms in e.g. DTBM-SEGPHOS.[10–12]

In 2005, Imamoto and co-workers reported the quinoxaline-based P-chirogenic bisphosphine ligand (*R*,*R*)-QuinoxP* (Figure 1B).[16] This ligand has shown high enantioselectivity for various asymmetric transformations.[20–30] We have recently reported new quinoxaline-based P-chirogenic bisphosphine ligands for the enantioselective Markovnikov hydroboration of aliphatic terminal alkenes.[31] Those ligands were obtained from the introduction of sterically bulky substituents on the phosphorus atoms, which was assisted by DFT calculations, i.e., improvement of ligand performance was achieved via synthetic modifications of the substituents on the phosphorus atoms.[32] However, the synthesis of the ligands is laborious, and the number of potential substructures on the phosphorus atoms is limited.

In the present study, we developed a novel series of high-performance C_2-symmetrical chiral bisphosphine ligand, (*R*,*R*)-5,8-*Si*-QuinoxP* [*Si* = trimethylsilyl (TMS) groups, triethylsilyl (TES) groups, or triisopropylsilyl (TIPS) groups] modified by the introduction of the silyl groups on the ligand backbone (Figure 1C, top).[33–36] The structures of these bisphosphines are characterized by interlocking structures between the substituents on the phosphorus atoms and the silyl groups introduced at the 5- and 8-positions of the quinoxaline backbone. We tested these ligands in the copper(I)-catalyzed direct enantioconvergent borylation of allyl electrophiles, which has previously been

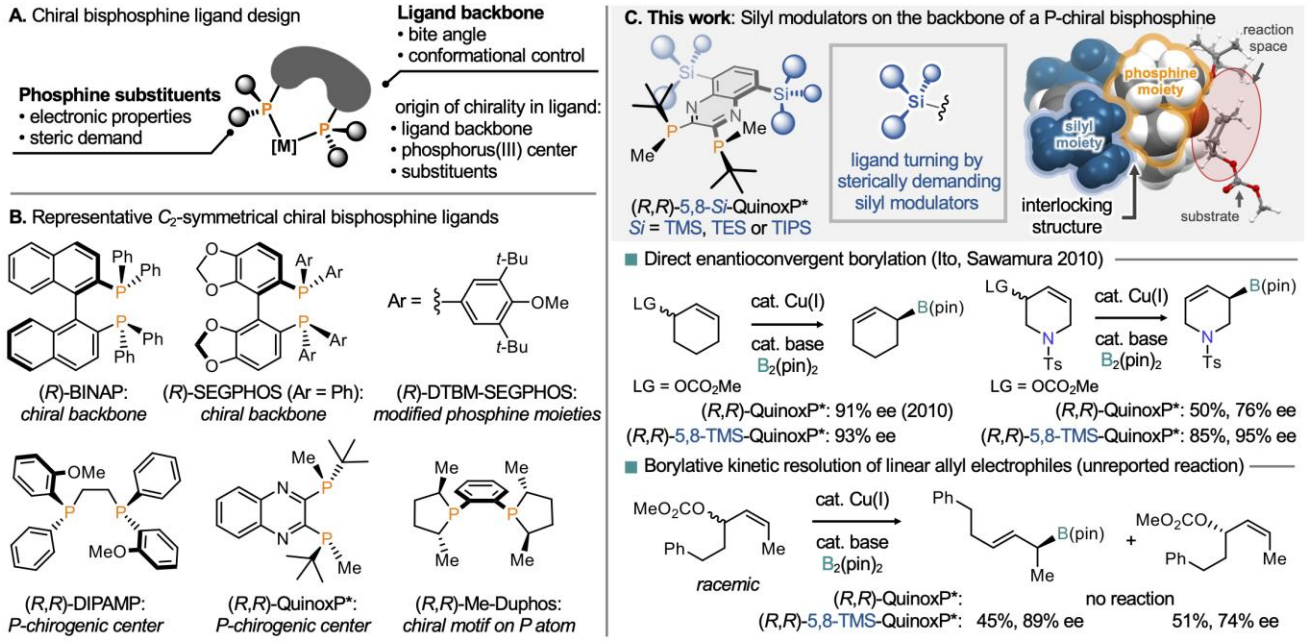

Figure 1. A novel series of C_2-symmetrical P-chirogenic bisphosphine ligands modified by the introduction of the silyl groups on the ligand backbone for the enantioselective borylation of racemic allyl electrophiles.

achieved by the parent ligand (*R*,*R*)-QuinoxP*, albeit that the substrate scope was limited. The ligand bearing TMS groups, (*R*,*R*)-5,8-TMS-QuinoxP*, showed higher reactivity and enantioselectivity for the copper(I)-catalyzed direct enantioconvergent borylation of heterocyclic allyl electrophiles than (*R*,*R*)-QuinoxP* (Figure 1C, middle).[24] Furthermore, we successfully developed a borylative kinetic resolution of linear allyl electrophiles using (*R*,*R*)-5,8-TMS-QuinoxP* (Figure 1C, bottom). A computational study investigating the effects of the sterically demanding silyl groups indicated that (*R*,*R*)-5,8-*Si*-QuinoxP* relatively destabilizes a dormant dimeric borylcopper(I) species in the catalytic cycle via the entropic effect. This effect can be expected to be important for the enhancement of the reactivity. Furthermore, detailed calculations of the transition state (TS) of the stereoselectivity-determining step revealed a strong enantioselective recognition of carbon–carbon double bonds, which is virtually unaffected by the chirality around the leaving group of the racemic substrates in the case of the direct enantioconvergent borylation.

RESULTS AND DISCUSSION

To implement the backbone modification strategy, we introduced sterically demanding silyl groups at the 5- and 8-positions of the quinoxaline backbone of (*R*,*R*)-QuinoxP* to afford the new series (*R*,*R*)-5,8-*Si*-QuinoxP* (Figure 2). The lithiation/silylation of 2,3-dichloroquinoxaline with lithium 2,2,6,6-tetramethyl piperidide (TMPLi) and the corresponding silyl electrophiles (R_3Si–X) was carried out according to the conditions used by Knochel and co-workers (Figure 2A).[37] The reaction of the resulting 5,8-disilyl-2,3-dichloroquinoxaline with the corresponding chiral phosphine-borane nucleophilic species, followed by deprotection of the borane group furnished the chiral bisphosphine ligand (*R*,*R*)-5,8-*Si*-QuinoxP*.[16,38] By using similar synthetic procedures, we prepared a series of novel chiral ligands, (*R*,*R*)-5,8-*Si*-QuinoxP* [*Si* = TMS, TES, or TIPS], which bear various sterically demanding silyl groups (Figures S1–S5). A single-crystal X-ray diffraction analysis revealed that (*R*,*R*)-5,8-TMS-QuinoxP* is entirely twisted with interlocking structures between the phosphine and silyl moieties on the ligand backbone (Figure 2B). To investigate the coordination behavior of this ligand toward transition metals, we then prepared a palladium(II) dichloride complex (Figure 2C). The solid-state structure of this palladium(II) complex also

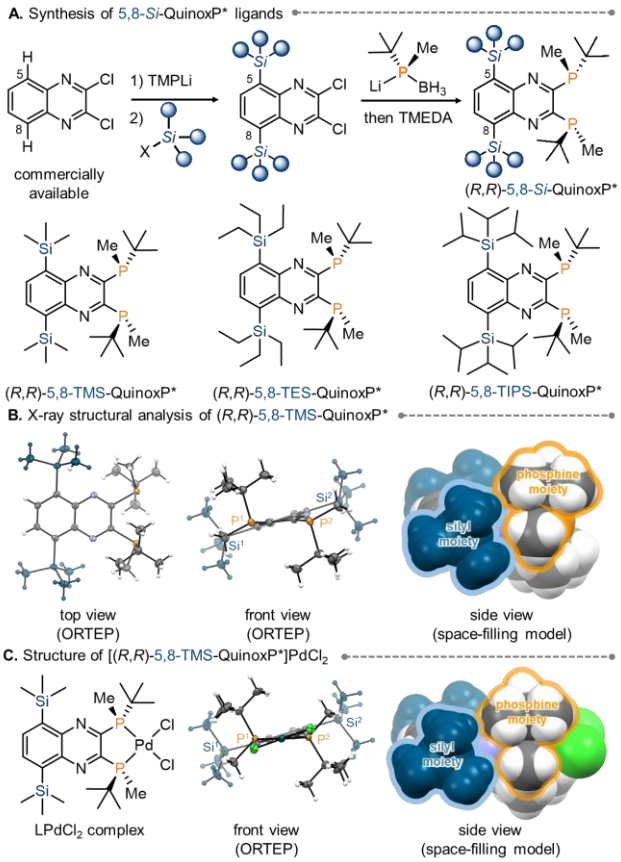

Figure 2. Synthesis and characterization of the silyl-modified QuinoxP*-type ligands (*R*,*R*)-5,8-*Si*-QuinoxP*.

indicated the presence of twisted molecular plane and interlocking structures between the silyl groups on the ligand and the phosphine substituents.

We then applied these modified ligands to the copper(I)-catalyzed direct enantioconvergent allylic borylation of racemic six-membered cyclic allyl electrophiles (**1**) in order to determine their effect on the catalytic performance (Table 1).[24,39,40–42] We have previously reported that the copper(I)-catalyzed direct enantioconvergent borylation using (*R*,*R*)-QuinoxP* can provide chiral allylboronates from racemic allyl electrophiles without an *in-situ* symmetrization. Regardless of the chirality of the substrate, a single enantiomer was obtained via the *anti*-S_N2' pathway and the *syn*-S_N2' pathway from both enantiomers. The direct enantioconvergent borylation of five-membered cyclic racemic allyl electrophiles under the reported reaction conditions with Cu(O-*t*-Bu) furnished the corresponding allylboronates in high yield (up to 98% yield with 97% ee). Conversely, the reaction of the six-membered cyclic allyl electrophile *rac*-**1a** showed lower enantioselectivity compared to that of five-membered allylic electrophiles (91% ee).[24] Moreover, there was only one example of the reaction of six-membered cyclic substrate *rac*-**1a**. In any case, the use of Cu(O-*t*-Bu), which is neither commercially available nor easy to handle, diminishes the utility of this reaction. However, the use of the commercially available copper(I) precursor $[Cu(MeCN)_4]BF_4$ resulted in low reactivity and enantioselectivity (entry 1: 12%, 79% ee). Therefore, we examined a series of silyl-modified ligands, (*R*,*R*)-5,8-*Si*-QuinoxP* [*Si* = TMS, TES, or TIPS] in the direct enantioconvergent borylation of *rac*-**1a** (entries 2–5). In the presence of (*R*,*R*)-5,8-TMS-QuinoxP*, the reactivity and enantioselectivity were improved, even when $[Cu(MeCN)_4]BF_4$ was used (entry 2: 92%, 93% ee). When (*R*,*R*)-5,8-TMS-QuinoxP* was tested under the conditions used for Cu(O-*t*-Bu), the enantioselectivity was higher than that using silyl-free (*R*,*R*)-QuinoxP* (entry 3: 77%, 94% ee).[24] The reaction using (*R*,*R*)-5,8-TES-QuinoxP* exhibited lower enantioselectivity, albeit that the reactivity was still high (entry 4: 94%, 85% ee). Conversely, the reaction using (*R*,*R*)-5,8-TIPS-QuinoxP* showed high reactivity and enantioselectivity (entry 5: 95%, 93% ee). We also examined several chiral bisphosphine ligands, i.e., (*R*)-SEGPHOS and (*R*,*R*)-Me-Duphos (entries 6 and 7). Both chiral bisphosphine ligands resulted in low enantioselectivity (entry 6: 57%, 25% ee; entry 7: 89%, 45% ee). Therefore, it is feasible to conclude that the presence of the silyl groups on the backbone of QuinoxP*-type ligands enhances the reactivity and enantioselectivity of the direct enantioconvergent borylation of the six-membered-ring substrate.

Table 1. Ligand Screening for the Direct Enantioconvergent Borylation of Racemic 1a.[a]

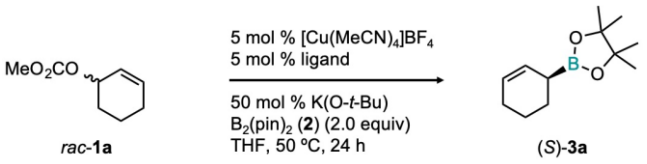

rac-**1a** (*S*)-**3a**

Entry	Ligand	conv. (%)[b]	yield (%)[b]	ee (%)[c]
1	(*R*,*R*)-QuinoxP*	39	12	79
2	(*R*,*R*)-5,8-TMS-QuinoxP*	94	92	93
3[d]	(*R*,*R*)-5,8-TMS-QuinoxP*	>95	77	94
4	(*R*,*R*)-5,8-TES-QuinoxP*	>95	94	85
5	(*R*,*R*)-5,8-TIPS-QuinoxP*	>95	95	93
6	(*R*)-SEGPHOS	92	57	25
7	(*R*,*R*)-Me-Duphos	94	89	45

[a]Conditions: $[Cu(MeCN)_4]BF_4$ (0.025 mmol), ligand (0.025 mmol), *rac*-**1a** (0.5 mmol), **2** (1.0 mmol), and K(O-*t*-Bu) (0.25 mmol) in THF (0.5 mL). [b]Yield and conversion values were determined by quantitative ^1H NMR analysis of the crude material using an internal standard. [c]Enantioselectivity values were determined by HPLC analysis after derivatization by allylboration of benzaldehyde with (*S*)-**3a**. [d]Conditions: Cu(O-*t*-Bu) (0.05 mmol), ligand (0.05 mmol), *rac*-**1a** (0.5 mmol), and **2** (0.75 mmol) in Et_2O (0.5 mL) at 30 °C.

Subsequently, we investigated the substrate scope of this direct enantioconvergent borylation with respect to racemic five-, six-, and seven-membered-ring substrates *rac*-**1**, including heterocycles, using (*R*,*R*)-5,8-TMS-QuinoxP* (Table 2). The effect of the silyl groups was also examined for each substrate *rac*-**1**. Allylboronate (*S*)-**3a** was obtained in high yield and enantioselectivity when (*R*,*R*)-5,8-TMS-QuinoxP* was used [(*R*,*R*)-5,8-TMS-QuinoxP*: 92%, 93% ee, (*R*,*R*)-QuinoxP*: 12%, 79% ee]. Furthermore, the reaction using (*R*,*R*)-5,8-TMS-QuinoxP* was applicable to heterocyclic substrates *rac*-**1b**–**1e**. Products including a piperidine structure with various protecting groups were also furnished in higher yield and excellent enantioselectivity compared to those using (*R*,*R*)-QuinoxP* [(*R*)-**3b**, (*R*,*R*)-5,8-TMS-QuinoxP*: 85%, 95% ee; (*R*,*R*)-QuinoxP*: 50%, 76% ee; (*R*)-**3c**, (*R*,*R*)-5,8-TMS-QuinoxP*: 84%, 90% ee; (*R*,*R*)-QuinoxP*: 67%, 83% ee; (*R*)-**3d**, (*R*,*R*)-5,8-TMS-QuinoxP*: 84%, 90% ee, (*R*,*R*)-QuinoxP*: 38%, 82% ee]. Moreover, the reaction of the dihydropyran-type substrate *rac*-**1e** afforded (*R*)-**3e** with high reactivity and excellent enantioselectivity, albeit that (*R*)-**3e** was slightly unstable toward purification on silica gel [(*R*,*R*)-5,8-TMS-QuinoxP*: 92%, 96% ee; (*R*,*R*)-QuinoxP*: 84%, 80% ee]. The reactivity of the products were slightly lower for dimethyl-moiety-bearing substrate *rac*-**1f**, whereas the use of (*R*,*R*)-QuinoxP* afforded only trace amounts of (*S*)-**3f** [(*R*,*R*)-5,8-TMS-QuinoxP*: 73%, 84% ee; (*R*,*R*)-QuinoxP*: <5%]. Furthermore, we tested *N*,*O*-acetal and acetal-type electrophiles *rac*-**1g** and *rac*-**1h** as substrates. The reaction of *N*,*O*-acetal *rac*-**1g** was carried out at low temperature (0 °C) due to the relatively high reactivity of the substrate. Even then, the enantioselectivity of enamine-bearing product (*S*)-**3g** was moderate (90%, 79% ee). However, the reactivity and enantioselectivity obtained for acetal-type substrate *rac*-**1h** were low (40%, 56% ee). (*R*,*R*)-QuinoxP* was not applicable for either *rac*-**1g** or *rac*-**1h** [(*S*)-**3g**: 10%; (*S*)-**3h**,: <5%]. These results clearly demonstrate the advantageous reactivity and enantioselectivity of 5,8-TMS-QuinoxP* relative to QuinoxP*.

Next, we examined the direct enantioconvergent borylation of five-membered-ring substrates using (*R*,*R*)-5,8-TMS-QuinoxP* and (*R*,*R*)-QuinoxP*. The reactions of the cyclopentenol derivative *rac*-**1i** using (*R*,*R*)-5,8-TMS-QuinoxP* or (*R*,*R*)-QuinoxP* resulted in similar yield and enantioselectivity of (*S*)-**3i** [(*R*,*R*)-5,8-TMS-QuinoxP*: 80%, 92% ee; (*R*,*R*)-QuinoxP*: 81%, 91% ee]. Although the reaction of the five-membered-ring racemic tertiary allyl alcohol substrate *rac*-**1j** with (*R*,*R*)-5,8-TMS-QuinoxP* provided the corresponding allylboronate (*S*)-**3j** with slightly lower enantioselectivity compared to (*R*,*R*)-QuinoxP*, the reactivity of the borylation using (*R*,*R*)-5,8-TMS-QuinoxP* was significantly higher than that of (*R*,*R*)-QuinoxP* [(*R*,*R*)-5,8-TMS-QuinoxP*: 92%, 94% ee; (*R*,*R*)-QuinoxP*: 48%, 97% ee]. In the case of the reaction of the seven-membered-ring substrate, *rac*-**1k**, (*R*,*R*)-5,8-TMS-QuinoxP* also showed higher reactivity and enantioselectivity

Table 2. Substrate Scope of the Direct Enantioconvergent Borylation with Respect to Racemic Substrates.[a]

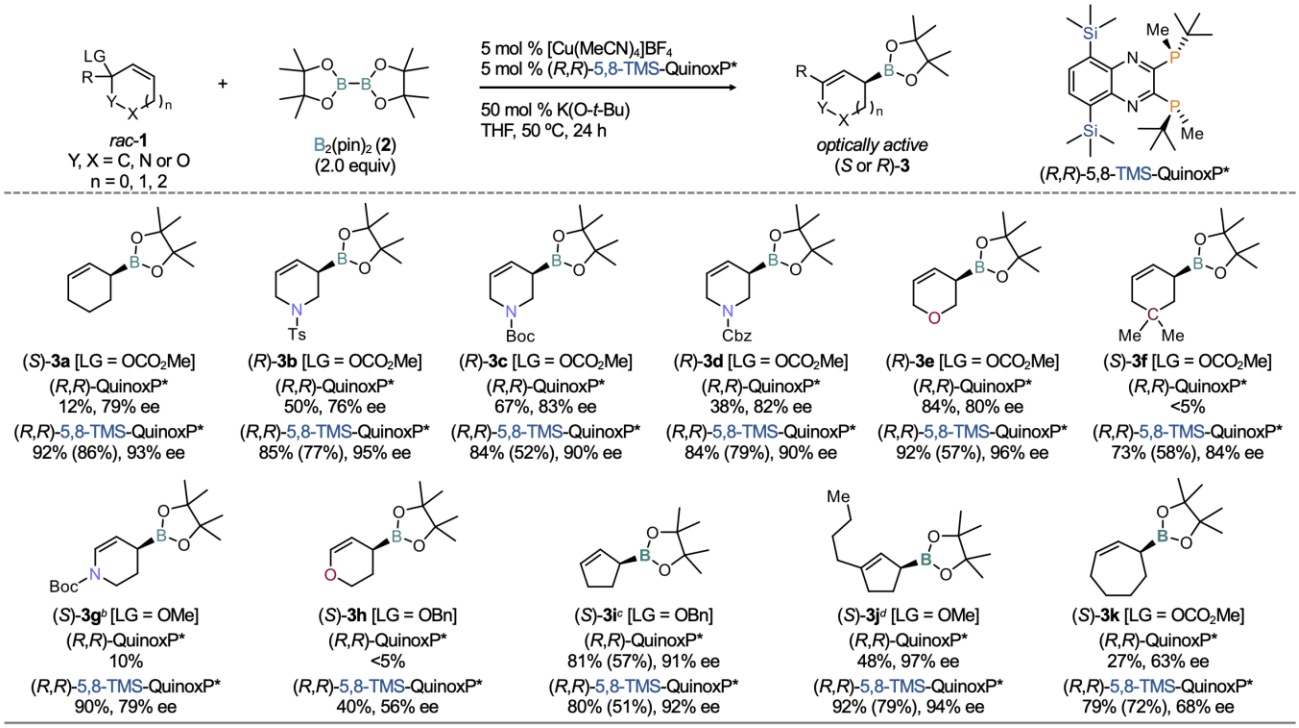

[a]Conditions: $[Cu(MeCN)_4]BF_4$ (0.025 mmol), ligand (0.025 mmol), *rac*-**1** (0.5 mmol), **2** (1.0 mmol), and K(O-*t*-Bu) (0.25 mmol) in THF (0.5 mL). Yield values were determined by quantitative ^1H NMR analysis of the crude material using an internal standard. Isolated yield values are shown in parentheses. Enantioselectivity values were determined by HPLC analysis after derivatization by allylboration of benzaldehyde with (*S* or *R*)-**3**. [b]Reaction temperature: 0 °C with 0.025 mmol of K(O-*t*-Bu) (5 mol %). [c]Reaction temperature: 0 °C with 0.25 mmol of K(O-*t*-Bu) (50 mol %). [d]Reaction temperature: 30 °C with 0.25 mmol of K(O-*t*-Bu) (50 mol %).

than (*R*,*R*)-QuinoxP*, albeit that the enantioselectivity was moderate [(*R*,*R*)-5,8-TMS-QuinoxP*: 79%, 68% ee; (*R*,*R*)-QuinoxP*: 27%, 63% ee].

As the QuinoxP*-type ligands showed strong prochiral face recognition for the alkene structure, we applied the current catalyst system to the reaction of the racemic linear allyl carbonates *rac*-(*Z*)-**4** (Table 3).[43] At first, we anticipated that the direct enantioconvergence would also proceed in the case of the linear allyl electrophiles. However, the reaction of *rac*-(*Z*)-**4** under the optimized conditions (Table 2) resulted only in moderate enantioselectivity (74%, 48% ee). Thus, we investigated the possibility of kinetic resolution of linear allyl electrophiles of the type *rac*-(*Z*)-**4**. Our modified ligand (*R*,*R*)-5,8-TMS-QuinoxP* exhibited high selectivity and reactivity for the borylative kinetic resolution of *rac*-(*Z*)-**4** at low temperature. The (*Z*)-allyl carbonates *rac*-(*Z*)-**4** were converted into the corresponding allylboronates (*S*,*E*)-**5** with high selectivity [(*S*,*E*)-**5a**: 42%, 86% ee, *s* = 21.2; (*S*,*E*)-**5b**: 45%, 89% ee, *s* = 16.9; (*S*,*E*)-**5c**: 51%, 83% ee, *s* = 21.3], while the allyl carbonates (*S*,*Z*)-**4** were recovered with moderate to high enantioselectivity [(*S*,*Z*)-**4a**: 58%, 63% ee; (*S*,*Z*)-**4b**: 51%, 74% ee; (*S*,*Z*)-**4c**: 44%, 92% ee].[44] Furthermore, substrates bearing linear alkyl chains and an *iso*-propyl group at the allylic position were also applicable to this kinetic resolution [(*S*,*E*)-**5d**: 45%, 88% ee; (*S*,*Z*)-**4d**: 45%, 81% ee, *s* = 12.0; (*S*,*E*)-**5e**: 36%, 88% ee; (*S*,*Z*)-**4e**: 51%, 55% ee, *s* = 6.3]. The reaction of a substrate including an acetal moiety gave the allylboronate in high enantioselectivity [(*S*,*E*)-**5f**: 42%, 90% ee, (*S*,*Z*)-**4f**: 57%, 69% ee, *s* = 46.4]. In contrast, (*R*,*R*)-QuinoxP* and (*R*,*R*)-BenzP* showed extremely low conversion of *rac*-(*Z*)-**4**.[45]

Table 3. Substrate Scope for the Asymmetric Borylative Kinetic Resolution of Linear Allyl Electrophiles 4.[a]

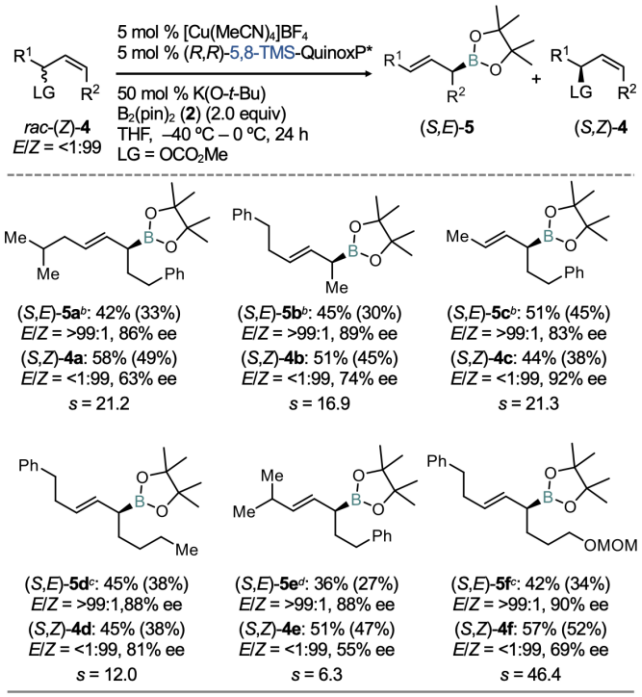

[a]Conditions: $[Cu(MeCN)_4]BF_4$ (0.025 mmol), ligand (0.025 mmol), *rac*-(*Z*)-**4** (0.5 mmol), **2** (1.0 mmol), and K(O-*t*-Bu) (0.25 mmol) in THF (0.5 mL) at –40 °C. Yield values were determined by

quantitative ^{1}H NMR analysis of the crude material using an internal standard. Isolated yield values are shown in parentheses. Enantioselectivity values were determined by HPLC analysis. Selectivity factor calculated from s = ln[(1–C)(1–ee)]/ln[(1–C)(1+ee)], where ee = ee(recovered substrate)/100 and C = conversion/100. [b]Reaction temperature: –40 °C. [c]Reaction temperature: –20 °C. [d]Reaction temperature: 0 °C.

As several of the allylboronates synthesized were unstable toward purification by column chromatography on silica gel, we carried out a subsequent borylation/allylboration of the aldehyde without quenching after the borylation (Figure 3A).[46–48] The corresponding chiral secondary alcohol (*S*,*S*)-**6**, bearing an unsaturated piperidine moiety, was obtained in high yield with excellent enantio- and diastereoselectivity (87% over two steps, 87% ee).[48] Subsequently, we carried out a direct enantioconvergent borylation of the deuterated allyl electrophile *rac*-**1a-D** to confirm whether this reaction proceeds without symmetrization i.e., via π-allyl metal species (Figure 3B). The reaction of *rac*-**1a-D** furnished the corresponding allylboronate (*S*)-**3a-D** with deuterium incorporation at the alkene position (84%, 93% ee), while a product with deuterium incorporated at the carbon bound to the boryl group was not detected. This result indicates that this reaction convergently and exclusively furnishes enantiomer (*S*)-**3a-D** without symmetrization via e.g. a π-allyl copper(III) intermediate.[49–52]

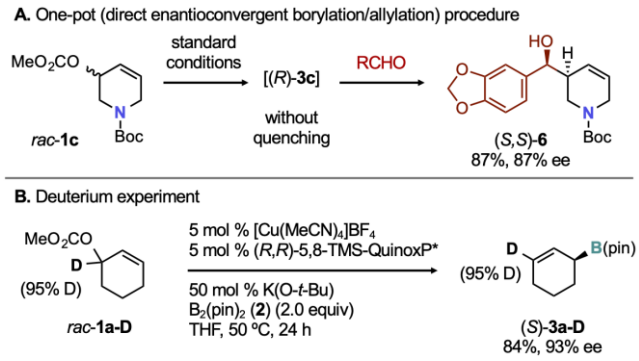

Figure 3. Synthetic applications and deuterium incorporation for the direct enantioconvergent borylation of *rac*-**1**.

A plausible reaction pathway for the copper(I)-catalyzed direct enantioconvergent borylation is shown in Figure 4A.[24,53–55] First, copper alkoxide **I** is formed from the cationic copper(I) precursor and a potassium alkoxide. A subsequent reaction of copper(I) alkoxide **I** with diboron **2** furnishes borylcopper(I) species **II**. The coordination of the substrate *rac*-**1a**, followed by the enantioselective borylcupration (**TS1**) of the carbon–carbon double bond, gives alkylcopper(I) intermediate **IV**. In this step, the catalyst mainly recognizes the alkene geometry and is not affected by the chiral center around the C–O bond of the allyl carbonate *rac*-**1a**. Both *anti*- and *syn*-elimination from the resulting mixture of diastereoisomers of the alkylcopper(I) intermediate convergently generate the single enantiomer (*S*)-**3a**. In addition, according to previously reported computational and experimental results, the dimers **V** of the borylcopper(I)-bisphosphine complexes **II** would be thermodynamically more stable than the corresponding monomers.[56,57] The borylcopper(I) dimers **V** can thus be considered a dormant species of the copper(I)/diboron catalytic borylation system.

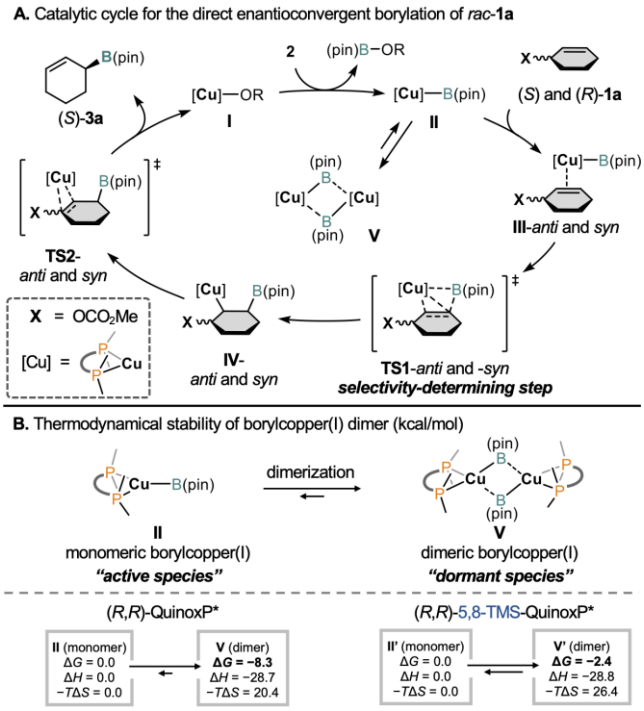

Figure 4. Proposed catalytic cycle and evaluation of potentially dormant species bearing (*R*,*R*)-QuinoxP* and (*R*,*R*)-5,8-TMS-QuinoxP*

We began investigating the effect of the silyl groups of (*R*,*R*)-5,8-TMS-QuinoxP* on the higher reactivity relative to (*R*,*R*)-QuinoxP* by an energetic analysis of borylcopper(I) dimers **V** using DFT calculations (Figure 4B). We compared the estimated thermodynamic stability of borylcopper(I) dimer complexes **V** and **V'**, which bear (*R*,*R*)-QuinoxP* and (*R*,*R*)-5,8-TMS-QuinoxP*, respectively. Similar to the previous report,[56] the relative Gibbs free energies (Δ*G*) of both dimeric species **V** and **V'** were lower than those of monomeric species **II** and **II'** [(*R*,*R*)-QuinoxP*, **V** (dimer): Δ*G* = –8.3 kcal/mol; (*R*,*R*)-5,8-TMS-QuinoxP*, **V'** (dimer): Δ*G* = –2.4 kcal/mol; Figure 4B]. Furthermore, the relative free energy of dimer **V'**, which bears (*R*,*R*)-5,8-TMS-QuinoxP*, was higher than that of the dimer **V**, which bears (*R*,*R*)-QuinoxP* (ΔΔ*G* = +5.9 kcal/mol). Although both relative enthalpy values (Δ*H*) of the dimeric species were almost identical [**V**: Δ*H* = –28.7 kcal/mol; **V'**: Δ*H* = –28.8 kcal/mol; ΔΔ*H* = –0.1 kcal/mol], the value of the term including the relative entropy (–*T*Δ*S*) for **V'** was significantly higher than that of **V** [**V**: –*T*Δ*S* = 20.4 kcal/mol; **V'**: –*T*Δ*S* = 26.4 kcal/mol; Δ(–*T*Δ*S*) = +6.0 kcal/mol]. Accordingly, the difference of the Gibbs free energy (Δ*G*) of the dimeric species strongly depends on the entropy factor (–*T*Δ*S*). This comparison suggests that the dimers would be relatively destabilized in the case of the reaction using (*R*,*R*)-5,8-TMS-QuinoxP*. This would lead to a higher concentration of the monomeric complex, which is an active species for the borylation, and thus enhance the reactivity. This is consistent with the experimentally observed higher reactivity of (*R*,*R*)-5,8-TMS-QuinoxP* (Table 2 and 3). Given that the entropy effect more strongly affected silyl-modified **V'** rather than **V**, we speculate that an inhibition of the free rotation of the silyl groups and phosphine substituents by the interlocking interactions in (*R*,*R*)-5,8-TMS-QuinoxP* potentially increases the value of (–*T*Δ*S*) to destabilize the dimeric species (for details, see Figures S6–S9, Tables S4–S6).

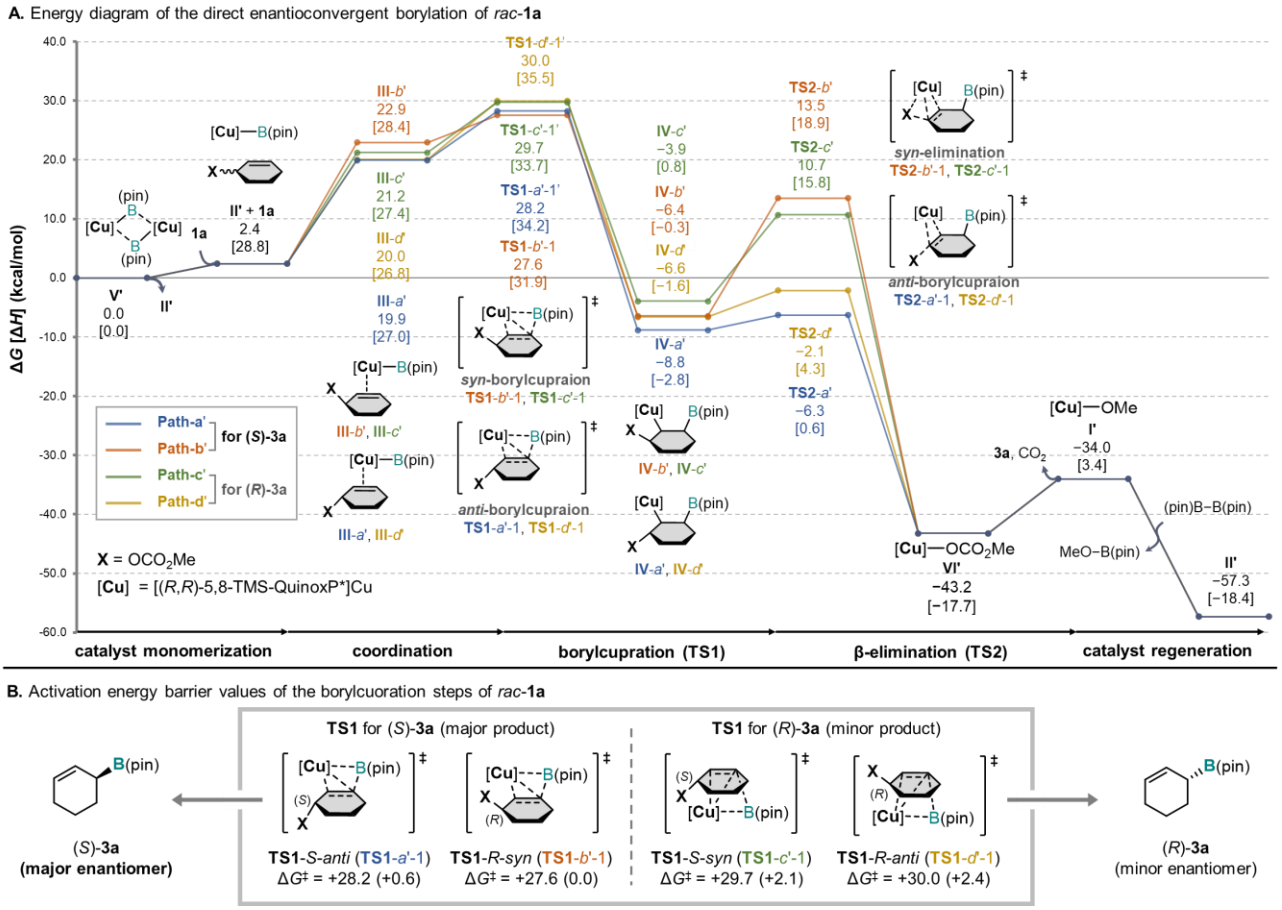

Figure 5. Energy diagram of reaction pathways of the direct enantioconvergent borylation of ***rac*-1a** and the activation Gibbs energy values ($\Delta G^{\ddagger}$) of the borylcupration step (**TS1**).

Next, we carried out DFT calculations on the reaction paths of the direct enantioconvergent borylation using (*R*,*R*)-5,8-TMS-QuinoxP* (Figure 5A). In the case of the direct enantioconvergent reaction of a racemic allyl electrophile with a C_2-symmetrical ligand, there are four possible reaction pathways: two paths via which (*R*)- or (*S*)-**1a** afford the major product (*S*)-**3a** [Figure 5A: path-*a*' and path-*b*'], and two via which they produce the minor product (*R*)-**3a** [Figure 5A: path-*c*' and path-*d*']. The calculated reaction pathways of *rac*-**1a**, including the borylcupration via **TS1** and the β-elimination via **TS2** suggest that all activation energies of **TS1** and **TS2** can be reached at the applied reaction temperature (50 °C), and that **TS1** should be the enantioselectivity-determining step because the borylcupration is irreversible. Furthermore, four types of TSs of the borylcupration of *rac*-**1a** (**TS1**) are conceivable: two transition states (TSs) affording (*S*)-**3a** via the *anti* or *syn*-borylcupration of (*S*)- or (*R*)-**1a**, respectively [Figure 5B: **TS1**-*S*-*anti* (**TS1**-*a*') and **TS1**-*R*-*syn* (**TS1**-*b*')], and two affording (*R*)-**3a** via the *syn* or *anti*-borylcupration of (*S*)- or (*R*)-**1a** [Figure 5B: **TS1**-*S*-*syn* (**TS1**-*c*') and **TS1**-*R*-*anti* (**TS1**-*d*')]. The analysis of the free activation energy values ($\Delta G^{\ddagger}$) of these four TSs (**TS1**-*a*'–*d*') showed that the **TS1** structures (**TS1**-*a*'-1: $\Delta G^{\ddagger}$ = 28.2 kcal/mol; **TS1**-*b*'-1: $\Delta G^{\ddagger}$ = 27.6 kcal/mol) for the major enantiomer (*S*)-**3a** are favored relative to those furnishing the minor product (*R*)-**3a** (**TS1**-*c*'-1: $\Delta G^{\ddagger}$ = 29.7 kcal/mol; **TS1**-*d*'-1: $\Delta G^{\ddagger}$ =30.0 kcal/mol). Conversely, the activation-energy barriers are not strongly affected by the geometry of the borylcupration (*syn* or *anti*). The results of our calculations thus suggest that the stereoselectivity of this direct enantioconvergent borylation is controlled by the strong enantioselective recognition of the prochiral alkene moiety, which does not depend on the allylic stereogenic center.[24] Furthermore, the Boltzmann-weighted average enantioselectivity of **TS1** (for details, see Figures S13 and S14) obtained from an exhaustive search for the **TS1** structures was in excellent agreement with the experimental value (ee_{pre}: 95% ee; ee_{exp}: 93% ee).[58]

In order to further improve our understanding of the mechanism of the enantioselectivity, we focused on the conformations of the bisphosphine ligand in the enantio-determining TS (**TS1**) because the conformation of chiral bisphosphines strongly relates to the chiral environment of the catalyst (Figure 6). An exhaustive structure search furnished 38 conformers of **TS1** (Figure S10). To categorize these structures, descriptors based on the dihedral angles formed by the corresponding bisphosphine–metal complex in the TS (Ψ_1 = C^1–C^2–P^2–[M]; Ψ_2: C^2–C^1–P^1–[M]) were defined.[59,60] The dihedral angles can be expected to describe a degree of twisting against the ligand backbone for each phosphine moiety. For example, a negative Ψ_1 value means that the *tert*-butyl group is inclined toward an axial position, while a positive Ψ_1 value means that the *tert*-butyl group is inclined toward an equatorial position (Figure 6A bottom).

Subsequently, we plotted the calculated activation-energy values ($\Delta G^{\ddagger}$) of all **TS1** conformations against both dihedral angle (Ψ) descriptors (Figure 6B). In this plot, the TS structures could be categorized into three discretely distributed groups.

The conformations of the phosphine moieties in these groups are represented by the combinations of the two dihedral angles (Ψ_1 and Ψ_2): 1) bottom-opened conformers with positive Ψ_1 and negative Ψ_2 ($\Psi_1 \gtrapprox 0$, $\Psi_2 < 0$) values; 2) top-opened conformers with negative Ψ_1 and positive Ψ_2 ($\Psi_1 < 0$, $\Psi_2 \gtrapprox 0$) values; 3) twisted conformers, in which both dihedral angles are negative ($\Psi_1 < 0$, $\Psi_2 < 0$). The lowest-energy TS structures of both racemic substrates for the major product (*S*)-**3a** (path-*a*' and path-*b*') were found in the twisted conformer group (**TS1**-*a*'-1: $\Delta G^{\ddagger}$ = +28.2 kcal/mol, Ψ_1 = –10.5°, Ψ_2 = –21.9°; **TS1**-*b*'-1: $\Delta G^{\ddagger}$ = +27.6 kcal/mol, Ψ_1 = –7.8°, Ψ_2 = –24.1°), while the lowest-energy TS structures for the minor product (*R*)-**3a** (path-*c*' and path-*d*') were found in the top-opened conformer group (**TS1**-*c*'-1: $\Delta G^{\ddagger}$ = +29.7 kcal/mol, Ψ_1 = –29.1°, Ψ_2 = 7.2°; **TS1**-*d*'-1: $\Delta G^{\ddagger}$ = +30.0 kcal/mol, Ψ_1 = –27.7°, Ψ_2 = 8.0°). The plot based on the dihedral angles (Ψ) and the activation-energy ($\Delta G^{\ddagger}$) thus indicates that the twisted conformer group represents a favored conformation for (*S*)-**3a**, and that the minor enantiomer (*R*)-**3a** would mainly be furnished from the TS structures in the top-opened conformer group. Interestingly, a distribution of the calculated TS structures with (*R*,*R*)-QuinoxP* in this plot was continuously linear, and the twisted conformer group was not found, which stands in contrast to those for (*R*,*R*)-5,8-TMS-QuinoxP* (for details, see Figure S22). Therefore, these results suggest that the dihedral angles (Ψ) can be used as a descriptor for the bisphosphines, and that there are conformational differences between (*R*,*R*)-5,8-TMS-QuinoxP* and (*R*,*R*)-QuinoxP* in the TS of the borylcupration.[60]

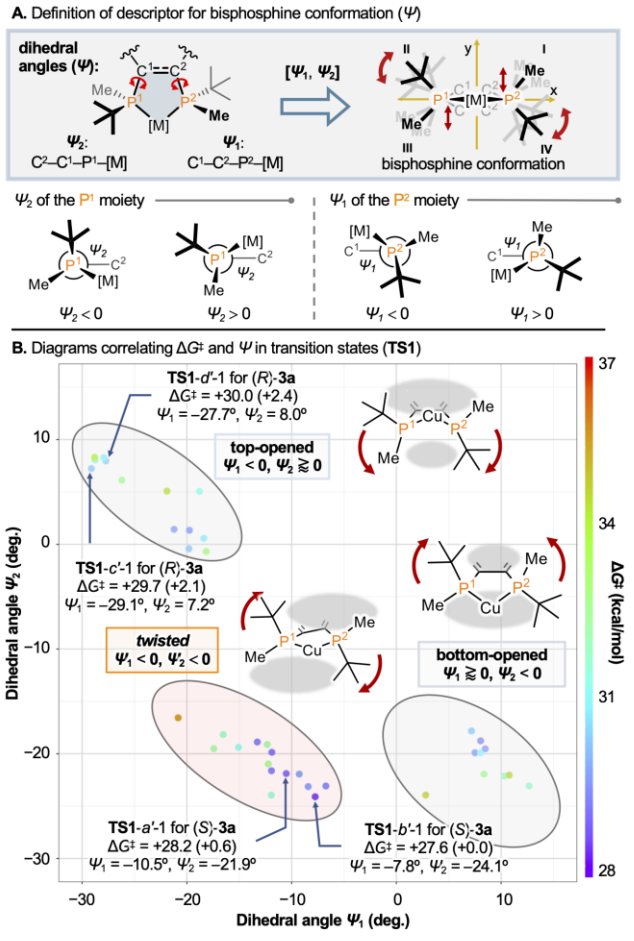

Figure 6. Relationship between the structure of the catalyst conformers and the activation Gibbs energy values ($\Delta G^{\ddagger}$) of the borylcupration step (**TS1**).

We conducted a distortion–interaction analysis (DIA) of the 38 calculated TS structures to quantitatively investigate the origin of the enantioselectivity (Figure 7).[61] The calculated distortion energies of a greater part of the TS structures for the major enantiomer (*S*)-**3a** (**TS1**-*a*' and **TS1**-*b*': E_{dist} > 44.4 kcal/mol) were smaller than those for minor enantiomers (**TS1**-*c*' and **TS1**-*d*': E_{dist} > 47.1 kcal/mol). Conversely, considerable differences were not found in the interaction energies between the TS structures for (*S*)-**3a** and (*R*)-**3a**. Therefore, this analysis also suggests that the enantioselectivity of this direct enantioconvergent borylation can be expected to be mainly controlled by the steric interactions that distort the ligand or substrate **1a** rather than the interactions between the catalyst and the substrate (for details, see Figures S13–S16).

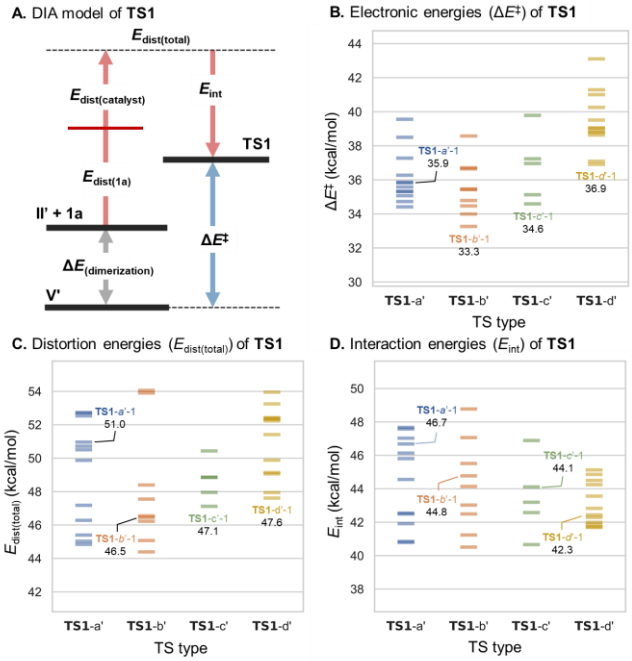

Figure 7. Distortion-interaction analysis (DIA) of the borylcupration step (**TS1**).

Finally, to investigate factors that affect the enantioselective recognition of the C–C double bond of racemic allyl carbonate **1a** by (*R*,*R*)-5,8-TMS-QuinoxP*, we focused on the TS structures with the lowest activation energies for each enantiomer in order to carry out a detailed structural analysis [**TS1**-*a*'-1 and **TS1**-*b*'-1 for (*S*)-**3a**; **TS1**-*c*'-1 and **TS1**-*d*'-1 for (*R*)-**3a**] (Figure 8). In the quadrant modeling of (*R*,*R*)-5,8-TMS-QuinoxP*, the twisted conformation is characterized by a bisphosphine conformation that exhibits large reaction spaces in quadrants **I** and **III**. Conversely, the top-opened conformation is characterized by a bisphosphine conformation that exhibits relatively large reaction spaces in quadrants **I** and **II**. In the TS structures categorized as a twisted conformer (**TS1**-*a*'-1 and **TS1**-*b*'-1), which give the major enantiomer (*S*)-**3a**, the allyl carbonate (*R*)- or (*S*)-**1a** was located in proximity to the large reaction space in quadrant **III** (Figures 8A and 8B). The B(pin) moieties are inclined and located in quadrant **I**, which is also sterically less hindered than quadrant **II**, to minimize steric repulsion between the B(pin) moieties and **1a**. The twisted conformers are able to afford (*S*)-**3a** because they provide sufficient reaction space for the cyclohexyl moieties and their leaving groups **X**, even in a *cis*-configuration (**TS1**-*b*'-1). Therefore, the enantioselectivity

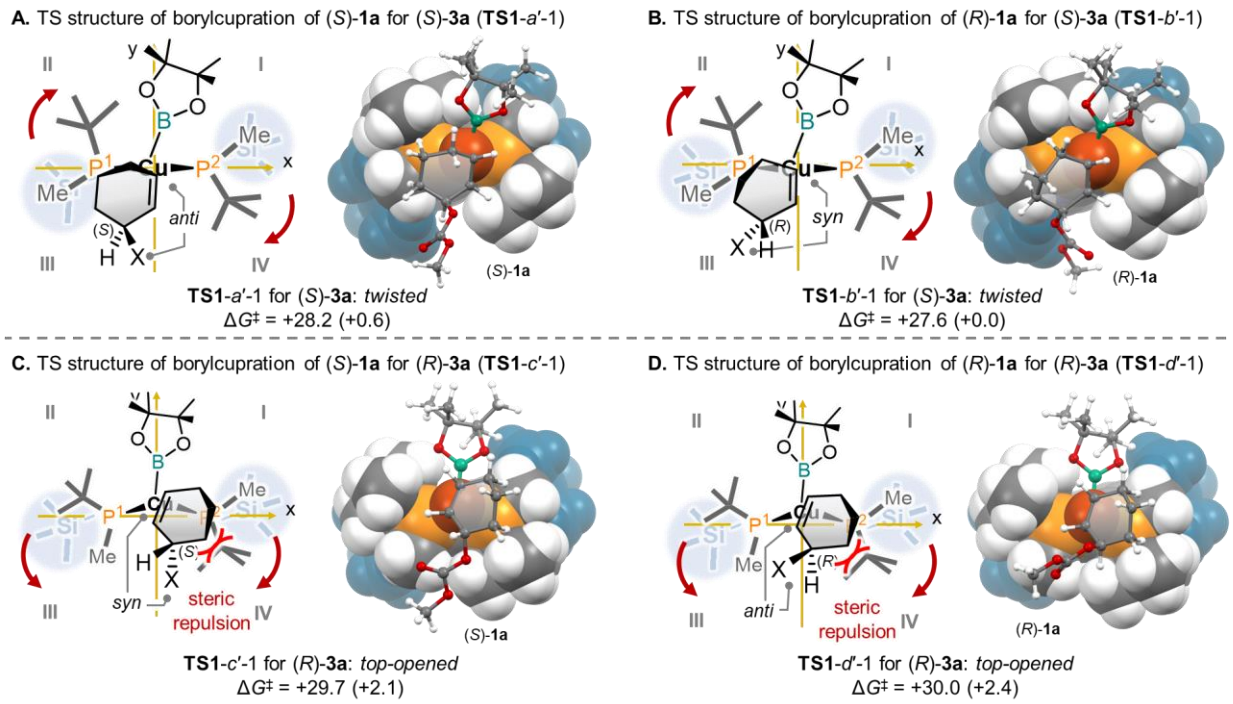

Figure 8. Detailed analysis of the lowest-energy transition state structures in each reaction paths (**TS1**-*a*'-1, **TS1**-*b*'-1, **TS1**-*c*'-1 and **TS1**-*d*'-1) with (*R*,*R*)-5,8-TMS-QuinoxP*. **X** = OCO_2Me.

of the reactions of both enantiomers of the substrate can be expected to be controlled only by the recognition of the prochiral C=C double bonds rather than by the substrate on the stereocenter via the leaving group **X**. In contrast, the lowest-energy TS structures that furnish the minor product (*R*)-**3a** for (*R*,*R*)-5,8-TMS-QuinoxP*, which are categorized as top-opened conformers (**TS1**-*c*'-1 and **TS1**-*d*'-1), would be destabilized by the steric interactions between the cyclohexyl moieties of the substrates and the *tert*-butyl group in quadrant **IV** (Figures 8C and 8D). The results of our DFT calculations on the reaction of acetal substrate *rac*-**1h**, which shows low enantioselectivity (56% ee), furthermore indicate that the steric demand of the substrate on the position adjacent to the leaving group located in quadrant **IV** is important for the enantioselective recognition (Figure S17).[62]

CONCLUSIONS

We have developed a novel series of chiral bisphosphine ligands, (*R*,*R*)-5,8-*Si*-QuinoxP*, modified by the introduction of the silyl moieties on the backbone. The ligand displays high performance in copper(I)-catalyzed direct enantioconvergent allylic borylation and borylative kinetic resolution reactions. The direct enantioconvergent allylic borylation using (*R*,*R*)-5,8-TMS-QuinoxP* converts racemic heterocyclic compounds into the corresponding allylboronate-functionalized heterocyclic compounds in high yield and enantioselectivity (up to 92% yield and 96% ee). Furthermore, the borylative kinetic resolution showed high *s* values for the chiral allylboronates (up to 90% ee, s = 46.4). A computational study of the effect of the silyl groups on the backbone in (*R*,*R*)-5,8-TMS-QuinoxP* by DFT calculations revealed that the rigid interlocking structure entropically destabilizes the borylcopper(I) dimer, which is a dormant species in the catalytic cycle, to enhance the reactivity. Further mechanistic studies indicated the highly selective direct enantioconvergent borylation is possible by the strong enantioselective recognition of the prochiral alkene moiety which does almost not depend on the chiral center at the allylic position. Efforts to apply the new chiral bisphosphine ligand to other enantioselective reactions, as well as to further develop backbone-modified P-chirogenic bisphosphine ligands, are currently in progress in our laboratory.

ASSOCIATED CONTENT

Supporting Information

The Supporting Information is available free of charge on the ACS Publications website.
Experimental procedure, compound characterization, NMR spectra, and computational data (PDF)
X-ray crystallography data (CIF)
Calculated structures (ZIP)

AUTHOR INFORMATION

Corresponding Author

* hajito@eng.hokudai.ac.jp

Author Contributions

The manuscript was written through contributions of all authors. All authors have given approval to the final version of the manuscript. #These authors contributed equally.

Notes

ORCIDs of the authors;
Hiroaki Iwamoto: 0000-0002-4771-1956
Yu Ozawa: 0000-0002-0299-7073
Tsuneo Imamoto: 0000-0003-3197-197X
Hajime Ito: 0000-0003-3852-6721

ACKNOWLEDGMENT

This work was financially supported by the Institute for Chemical Reaction Design and Discovery (WPI-ICReDD), which was established by the World Premier International Research Initiative (WPI), MEXT, Japan, as well as by JSPS KAKENHI grants 17H06370 and 18H03907. H. Iwamoto would like to thank the JSPS for a scholarship (16J01410). Y. O. would like to thank the JSPS for a scholarship (19J20823) and the "Program for Leading Graduate Schools" (Hokkaido University "Ambitious Leaders Program"). We thank Nippon Chemical Industrial Co., Ltd. for providing the chiral bisphosphine ligands. We thank Dr. Tomohiro Seki, Dr. Mingoo Jin, Mr. Koh Kobayashi and Mr. Kentaro Ida for the X-ray analysis. Parts of the computational calculations were carried out on the supercomputer of Research Center for Computational Science, Okazaki, Japan.

REFERENCES

(1) Phosphorus Ligands in Asymmetric Catalysis: Synthesis and Application; Börner, A., Ed.; Wiley-VCH: Weinheim, 2008; Vol. 1–3.
(2) Privileged Chiral Ligands and Catalysts; Zhou, Q.-L., Ed.; Wiley-VCH: Weinheim, 2011.
(3) Phosphorus(III) Ligands in Homogeneous Catalysis Design and Synthesis; Kamer, P. C. J., van Leeuwen, P. W. N. M., Eds.; Wiley-VCH: Weinheim, 2012.
(4) *Ligand Design in Metal Chemistry: Reactivity and Catalysis*; Stradiotto, M., Lundgren, R. J., Eds.; Wiley-VCH: Weinheim, 2016.
(5) Van Leeuwen, P. W. N. M.; Kamer, P. C. J.; Reek, J. N. H.; Dierkes, P. Ligand Bite Angle Effects in Metal-Catalyzed C–C Bond Formation. *Chem. Rev.* **2000**, *100*, 2741–2769.
(6) O'Neill, M. J.; Riesebeck, T.; Cornella, J. Thorpe–Ingold Effect in Branch-Selective Alkylation of Unactivated Aryl Fluorides. *Angew. Chem., Int. Ed.* **2018**, *57*, 9103–9107.
(7) Wagner, J. P.; Schreiner, P. R. London Dispersion in Molecular Chemistry - Reconsidering Steric Effects, *Angew. Chem., Int. Ed.* **2015**, *54*, 12274–12296.
(8) Liu, J.; Nie, M.; Zhou, Q.; Gao, S.; Jiang, W.; Chung, L. W.; Tang, W.; Ding, K. Enantioselective Palladium-Catalyzed Diboration of 1,1-Disubstituted Allenes. *Chem. Sci.* **2017**, *8*, 5161–5165.
(9) Lu, G.; Liu, R. Y.; Yang, Y.; Fang, C.; Lambrecht, D. S.; Buchwald, S. L.; Liu, P. Ligand-Substrate Dispersion Facilitates the Copper-Catalyzed Hydroamination of Unactivated Olefins. *J. Am. Chem. Soc.* **2017**, *139*, 16548–16555.
(10) Noyori, R. Asymmetric catalysis: Science and Opportunities (Nobel Lecture). *Angew. Chem., Int. Ed.* **2002**, *41*, 2008–2022.
(11) Berthod, M.; Mignani, G.; Woodward, G.; Lemaire, M. Modified BINAP: The How and the Why. *Chem. Rev.* **2005**, *105*, 1801–1836.
(12) Shimizu, H.; Nagasaki, I.; Matsumura, K.; Sayo, N.; Saito, T. Developments in Asymmetric Hydrogenation from an Industrial Perspective. *Acc. Chem. Res.* **2007**, *40*, 1385–1393.
(13) Knowles, W. S. Asymmetric Hydrogenations (Nobel Lecture). *Angew. Chem., Int. Ed.* **2002**, *41*, 1998–2007.
(14) Imamoto, T. Searching for Practically Useful P-Chirogenic Phosphine Ligands. *Chem. Rec.* **2016**, *16*, 2659–2673.
(15) Dutartre, M.; Bayardon, J.; Jugé, S. Applications and Stereoselective Syntheses of P-chirogenic Phosphorus Compounds. *Chem. Soc. Rev.* **2016**, *45*, 5771–5794.
(16) Imamoto, T.; Sugita, K.; Yoshida, K. An Air-Stable P-Chiral Phosphine Ligand for Highly Enantioselective Transition-Metal-Catalyzed Reactions. *J. Am. Chem. Soc.* **2005**, *127*, 11934–11935.
(17) Burk, M. J. C_2-Symmetric Bis(phospholanes) and Their Use in Highly Enantioselective Hydrogenation Reactions. *J. Am. Chem. Soc.* **1991**, *113*, 8518–8519.
(18) Burk, M. J.; Feaster, J. E.; Nugent, W. A.; Harlow, R. L. Preparation and Use of C_2-symmetric Bis(phospholanes): Production of α-Amino Acid Derivatives via Highly Enantioselective Hydrogenation Reactions. *J. Am. Chem. Soc.* **1993**, *115*, 10125–10138.
(19) Burk, M. J. Modular Phospholane Ligands in Asymmetric Catalysis. *Acc. Chem. Res.* **2000**, *33*, 363–372.
(20) Imamoto, T.; Nishimura, M.; Koide, A.; Yoshida, K. *t*-Bu-QuinoxP* Ligand: Applications in Asymmetric Pd-catalyzed Allylic Substitution and Ru-Catalyzed Hydrogenation. *J. Org. Chem.* **2007**, *72*, 7413–7416.
(21) Ito, H.; Ito, S.; Sasaki, Y.; Matsuura, K.; Sawamura, M. Copper-Catalyzed Enantioselective Substitution of Allylic Carbonates with Diboron: An Efficient Route to Optically Active α-Chiral Allylboronates. *J. Am. Chem. Soc.* **2007**, *129*, 14856–14857.
(22) Ito, H.; Kosaka, Y.; Nonoyama, K.; Sasaki, Y.; Sawamura, M. Synthesis of Optically Active Boron-Silicon Bifunctional Cyclopropane Derivatives through Enantioselective Copper(I)-Catalyzed Reaction of Allylic Carbonates with a Diboron Derivative. *Angew. Chem., Int. Ed.* **2008**, *47*, 7424–7427.
(23) Shibata, Y.; Tanaka, K. Rhodium-Catalyzed Highly Enantioselective Direct Intermolecular Hydroacylation of 1,1-Disubstituted Alkenes with Unfunctionalized Aldehydes. *J. Am. Chem. Soc.* **2009**, *131*, 12552–12553.
(24) Ito, H.; Kunii, S.; Sawamura, M. Direct Enantio-Convergent Transformation of Racemic Substrates without Racemization or Symmetrization. *Nat. Chem.* **2010**, *2*, 972–976.
(25) Yanagisawa, A.; Takeshita, S.; Izumi, Y.; Yoshida, K. Enantioselective Nitroso Aldol Reaction Catalyzed by QuinoxP*·Silver(I) Complex and Tin Methoxide. *J. Am. Chem. Soc.* **2010**, *132*, 5328–5329.
(26) Friedfeld, M. R.; Shevlin, M.; Hoyt, J. M.; Krska, S. W.; Tudge, M. T.; Chirik, P. J. Cobalt Precursors for High-Throughput Discovery of Base Metal Asymmetric Alkene Hydrogenation Catalysts. *Science* **2013**, *342*, 1076–1080.
(27) Li, H.; Belyk, K. M.; Yin, J.; Chen, Q.; Hyde, A.; Ji, Y.; Oliver, S.; Tudge, M. T.; Campeau, L.-C.; Campos, K. R. Enantioselective Synthesis of Hemiaminals via Pd-Catalyzed C–N Coupling with Chiral Bisphosphine Mono-Oxides. *J. Am. Chem. Soc.* **2015**, *137*, 13728–13731.
(28) Yu, S.; Wu, C.; Ge, S. Cobalt-Catalyzed Asymmetric Hydroboration/Cyclization of 1,6-Enynes with Pinacolboranes. *J. Am. Chem. Soc.* **2017**, *139*, 6526–6529.
(29) Chen, J.; Zhang, Z.; Li, B.; Li, F.; Wang, Y.; Zhao, M.; Gridnev, I. D.; Imamoto, T.; Zhang, W. $Pd(OAc)_2$-Catalyzed Asymmetric Hydrogenation of Sterically Hindered *N*-Tosylimines, *Nat. Commun.* **2018**, *9*, 5000.
(30) Li, B.; Chen, J.; Zhang, Z.; Gridnev, I. D.; Zhang, W. Ni-Catalyzed Asymmetric Hydrogenation of *N*-Sulfonyl Imines. *Angew. Chem., Int. Ed.* **2019**, *58*, 7329–7334.
(31) Iwamoto, H.; Imamoto, T.; Ito, H. Computational Design of High-performance Ligand for Enantioselective Markovnikov Hydroboration of Aliphatic Terminal Alkenes. *Nat. Commun.* **2018**, *9*, 2290.
(32) Iwamoto, H.; Endo, K.; Ozawa, Y.; Watanabe, Y.; Kubota, K.; Imamoto, T.; Ito, H. Copper(I)-Catalyzed Enantioconvergent Borylation of Racemic Benzyl Chlorides Enabled by Quadrant-by-Quadrant Structure Modification of Chiral Bisphosphine Ligands. *Angew. Chem., Int. Ed.* **2019**, *58*, 11112–11117.
(33) Hu, A.; Ngo, H. L.; Lin, W. Remarkable 4,4′-Substituent Effects on Binap: Highly Enantioselective Ru Catalysts for Asymmetric Hydrogenation of β-Aryl Ketoesters and Their Immobilization in Room-temperature Ionic Liquids. *Angew. Chem., Int. Ed.* **2004**, *43*, 2501–2504.
(34) Hu, A.; Ngo, H. L.; Lin, W. 4,4′-Disubstituted BINAPs for Highly Enantioselective Ru-Catalyzed Asymmetric Hydrogenation of Ketones. *Org. Lett.* **2004**, *6*, 2937–2940.
(35) Ogasawara, M.; Ngo, H. L.; Sakamoto, T.; Takahashi, T.; Lin, W. Applications of 4,4′-$(Me_3Si)_2$-BINAP in Transition-Metal-Catalyzed Asymmetric Carbon−Carbon Bond-Forming Reactions. *Org. Lett.* **2005**, *7*, 2881–2884.
(36) Storch, G.; Trapp, O. Temperature-Controlled Bidirectional Enantioselectivity in a Dynamic Catalyst for Asymmetric Hydrogenation. *Angew. Chem., Int. Ed.* **2015**, *54*, 3580–3586.
(37) Nafe, J.; Herbert, S.; Auras, F.; Karaghiosoff, K.; Bein, T.; Knochel, P. Functionalization of Quinoxalines by Using TMP Bases: Preparation of Tetracyclic Heterocycles with High Photoluminescene Quantum Yields. *Chem. - Eur. J.* **2015**, *21*, 1102–1107.
(38) Zhang, Z.; Tamura, K.; Mayama, D.; Sugiya, M.; Imamoto, T. Three-Hindered Quadrant Phosphine Ligands with an Aromatic Ring Backbone for the Rhodium-Catalyzed Asymmetric Hydrogenation of Functionalized Alkenes. *J. Org. Chem.* **2012**, *77*, 4184–4188.

(39) Mohr, J. T.; Moore, J. T.; Stoltz, B. M. Enantioconvergent Catalysis, *Beilstein J. Org. Chem.* **2016**, *12*, 2038–2045.
(40) Delvos, L. B.; Oestreich, M. Temperature-Dependent Direct Enantioconvergent Silylation of a Racemic Cyclic Allylic Phosphate by Copper(I)-Catalyzed Allylic Substitution. *Synthesis* **2015**, *47*, 924–933.
(41) Bohan, P. T.; Toste, F. D. Well-Defined Chiral Gold(III) Complex Catalyzed Direct Enantioconvergent Kinetic Resolution of 1,5-Enynes. *J. Am. Chem. Soc.* **2017**, *139*, 11016–11019.
(42) Ge, Y.; Cui, X. Y.; Tan, S. M.; Jiang, H.; Ren, J.; Lee, N.; Lee, R.; Tan, C. H. Guanidine–Copper Complex Catalyzed Allylic Borylation for the Enantioconvergent Synthesis of Tertiary Cyclic Allylboronates. *Angew. Chem., Int. Ed.* **2019**, *58*, 2382–2386.
(43) Ito, H.; Kawakami, C.; Sawamura, M. Copper-Catalyzed γ-Selective and Stereospecific Substitution Reaction of Allylic Carbonates with Diboron: Efficient Route to Chiral Allylboron Compounds. *J. Am. Chem. Soc.* **2005**, *127*, 16034–16035.
(44) The perfect *E*/*Z*-selectivity of this borylative kinetic resolution stands in sharp contrast to that of the copper(I)-catalyzed enantioselective alkylation of linear allyl electrophiles; for details, see: Langlois, J. B.; Alexakis, A. Identification of a Valuable Kinetic Process in Copper-Catalyzed Asymmetric Allylic Alkylation. *Angew. Chem., Int. Ed.* **2011**, *50*, 1877–1881.
(45) Imamoto, T.; Tamura, K.; Zhang, Z.; Horiuchi, Y.; Sugiya, M.; Yoshida, K.; Yanagisawa, A.; Gridnev, I. D. Rigid P-Chiral Phosphine Ligands with *tert*-Butylmethylphosphino Groups for Rhodium-Catalyzed Asymmetric Hydrogenation of Functionalized Alkenes. *J. Am. Chem. Soc.* **2012**, *134*, 1754–1769.
19)
(46) Lessard, S.; Peng, F.; Hall, D. G. α-Hydroxyalkyl Heterocycles via Chiral Allylic Boronates: Pd-Catalyzed Borylation Leading to a Formal Enantioselective Isomerization of Allylic Ether and Amine. *J. Am. Chem. Soc.* **2009**, *131*, 9612–9613.
(47) Diner, C.; Szabó, K. J. Recent Advances in the Preparation and Application of Allylboron Species in Organic Synthesis. *J. Am. Chem. Soc.* **2017**, *139*, 2–14.
20)
(48) The slight enantioselectivity erosion compared to the results of (*R*)-**3c** should be caused by a small amount of remaining substrate or catalyst.
(49) Goering, H. L.; Singleton, V. D. On the Stereochemistry of Conversion of Allylic Esters to Olefins with Lithium Dialkylcuprates. *J. Am. Chem. Soc.* **1976**, *98*, 7854–7855.
(50) Yamanaka, M.; Kato, S.; Nakamura, E. Mechanism and Regioselectivity of Reductive Elimination of π-Allylcopper (III) Intermediates. *J. Am. Chem. Soc.* **2004**, *126*, 6287–6293.
(51) Langlois, J. B.; Emery, D.; Mareda, J.; Alexakis, A. Mechanistic Identification and Improvement of a Direct Enantioconvergent Transformation in Copper-Catalyzed Asymmetric Allylic Alkylation. *Chem. Sci.* **2012**, *3*, 1062–1069.
(52) Rideau, E.; You, H.; Sidera, M.; Claridge, T. D. W.; Fletcher, S. P. Mechanistic Studies on a Cu-Catalyzed Asymmetric Allylic Alkylation with Cyclic Racemic Starting Materials. *J. Am. Chem. Soc.* **2017**, *139*, 5614–5624.
(53) Park, J. K.; Lackey, H. H.; Ondrusek, B. A.; McQuade, D. T. Stereoconvergent Synthesis of Chiral Allylboronates from an E/Z Mixture of Allylic Aryl Ethers Using a 6-NHC-Cu(I) Catalyst. *J. Am. Chem. Soc.* **2011**, *133*, 2410–2413.
(54) Guzman-Martinez, A.; Hoveyda, A. H. Enantioselective Synthesis of Allylboronates Bearing a Tertiary or Quaternary B-Substituted Stereogenic Carbon by NHC-Cu-Catalyzed Substitution Reactions. *J. Am. Chem. Soc.* **2010**, *132*, 10634–10637.
(55) Yamamoto, E.; Takenouchi, Y.; Ozaki, T.; Miya, T.; Ito, H. Copper(I)-Catalyzed Enantioselective Synthesis of α-Chiral Linear or Carbocyclic (*E*)-(γ-Alkoxyallyl)boronates. *J. Am. Chem. Soc.* **2014**, *136*, 16515–16521.
(56) Tobisch, S. Copper-Catalysed Aminoboration of Vinylarenes with Hydroxylamine Esters-A Computational Mechanistic Study. *Chem. - Eur. J.* **2017**, *23*, 17800–17809.
(57) Borner, C.; Anders, L.; Brandhorst, K.; Kleeberg, C. Elusive Phosphine Copper(I) Boryl Complexes: Synthesis, Structures, and Reactivity. *Organometallics* **2017**, *36*, 4687–4690.
(58) The DFT calculation of the borylcupration steps of the borylative kinetic resolution was also in good agreement with the experimental results. For details, see in the Supporting Information (Figure S18).
(59) Durand, D. J.; Fey, N. Computational Ligand Descriptors for Catalyst Design. *Chem. Rev.* **2019**, *119*, 6561–6594.
(60) This classification produced results similar to the clustering based on the atom coordinates of the catalyst structures in the TSs by clustering. Detailed results and discussions regarding the analysis are summarized in the Supporting Information (Figures S23–S29).
(61) Bickelhaupt, F. M.; Houk, K. N. Analyzing Reaction Rates with the Distortion/Interaction-Activation Strain Model. *Angew. Chem., Int. Ed.* **2017**, *56*, 10070–10086.
(62) Although having carried out a series of computational studies, we could not unequivocally reveal the effects of the silyl groups of the ligand backbone on the improvement of the enantioselectivity, given the relatively small difference of the selectivity for *rac*-**1a** between the parent ligand and the new ligand. However, our computational studies strongly suggest that the silyl groups of the backbone are not without influence on the catalyst conformation.

Insert Table of Contents artwork here